Cell Metabolism
Article

Non-CpG Methylation of the *PGC-1α* Promoter through DNMT3B Controls Mitochondrial Density

Romain Barrès,[1] Megan E. Osler,[1] Jie Yan,[1] Anna Rune,[1] Tomas Fritz,[3] Kenneth Caidahl,[2] Anna Krook,[1,4] and Juleen R. Zierath[1,4,*]
[1]Department of Molecular Medicine and Surgery, Section for Integrative Physiology
[2]Department of Molecular Medicine and Surgery, Section for Clinical Physiology
[3]Centre of Family Medicine
Karolinska University Hospital, Karolinska Institutet, Stockholm, Sweden
[4]Department of Physiology and Pharmacology, Karolinska Institutet, Stockholm, Sweden
*Correspondence: juleen.zierath@ki.se
DOI 10.1016/j.cmet.2009.07.011

SUMMARY

Epigenetic modification through DNA methylation is implicated in metabolic disease. Using whole-genome promoter methylation analysis of skeletal muscle from normal glucose-tolerant and type 2 diabetic subjects, we identified cytosine hypermethylation of peroxisome proliferator-activated receptor γ (PPARγ) coactivator-1 α (PGC-1α) in diabetic subjects. Methylation levels were negatively correlated with *PGC-1α* mRNA and mitochondrial DNA (mtDNA). Bisulfite sequencing revealed that the highest proportion of cytosine methylation within *PGC-1α* was found within non-CpG nucleotides. Non-CpG methylation was acutely increased in human myotubes by exposure to tumor necrosis factor-α (TNF-α) or free fatty acids, but not insulin or glucose. Selective silencing of the DNA methyltransferase 3B (*DNMT3B*), but not *DNMT1* or *DNMT3A*, prevented palmitate-induced non-CpG methylation of *PGC-1α* and decreased mtDNA and *PGC-1α* mRNA. We provide evidence for *PGC-1α* hypermethylation, concomitant with reduced mitochondrial content in type 2 diabetic patients, and link DNMT3B to the acute fatty-acid-induced non-CpG methylation of *PGC-1α* promoter.

INTRODUCTION

Type 2 diabetes mellitus (T2DM) and its associated metabolic consequences, such as kidney and heart failure, are leading causes of morbidity and mortality worldwide. T2DM is a chronic disorder characterized by insulin resistance in adipose tissue, liver, and skeletal muscle, which are metabolic organs affected by an impaired insulin secretion of the β-pancreatic cell. In particular, defects in skeletal muscle metabolism play a primary role in the development of whole-body insulin resistance (Eriksson et al., 1989), as this tissue is the major site of insulin-mediated glucose disposal (DeFronzo et al., 1985). The mechanisms underlying insulin resistance and T2DM are incompletely understood, but genetic and environmental factors such as physical activity and diet/nutrition are involved.

Epigenetic modifications of the genome, including DNA methylation, provide a potential molecular basis for the interaction between genetic and environmental factors on glucose homeostasis and may contribute to the manifestation of T2DM. Dietary factors that affect the activity of enzymes supplying methyl groups can influence the rate of disease manifestation (Van den Veyver, 2002). Evidence for a nutritional effect on epigenetic regulation in T2DM is suggested by a generational study in humans showing that the nutritional status of the parent is closely linked with an increased risk of T2DM-associated mortality in the second generation, raising the possibility of a role for epigenetic modifications of genomic DNA in metabolic disease (Pembrey et al., 2006). The impact of nutrition on DNA methylation has been directly shown in the *agouti* mice, whereby methyl donor supplementation prevented DNA hypomethylation of the intracisternal A particle retroviral element into the *agouti* gene of the offspring (Cooney et al., 2002; Michaud et al., 1994; Morgan et al., 1999). Whether epigenetic modifications acutely occur in somatic tissues of mammalian origin is unknown.

Here, we performed a genome-wide promoter analysis of DNA methylation to screen for genes differentially methylated in T2DM. We identified hypermethylation of genes involved in mitochondrial function, such as the peroxisome proliferator-activated receptor γ (PPARγ) coactivator-1 α (PGC-1α), and provide a mechanism by which elevations in cytokines or lipids induce non-CpG methylation of the PGC-1α promoter in skeletal muscle. Our results provide insight into the acute reprogramming of gene expression through methylation in metabolic disease.

RESULTS

Differential Methylation of *PGC-1α* Promoter in T2DM

We used methylated DNA immunoprecipitation (MeDIP), combined with microarray technology (Keshet et al., 2006; Weber et al., 2005), to discover whether changes in DNA methylation are specific to T2DM. A cohort of normal glucose-tolerant (NGT) and T2DM male volunteers was studied. The metabolic characteristics are presented in the Supplemental Data (Table S1). Importantly, we studied closely age-matched groups to exclude any possible effect of aging, since aging has been

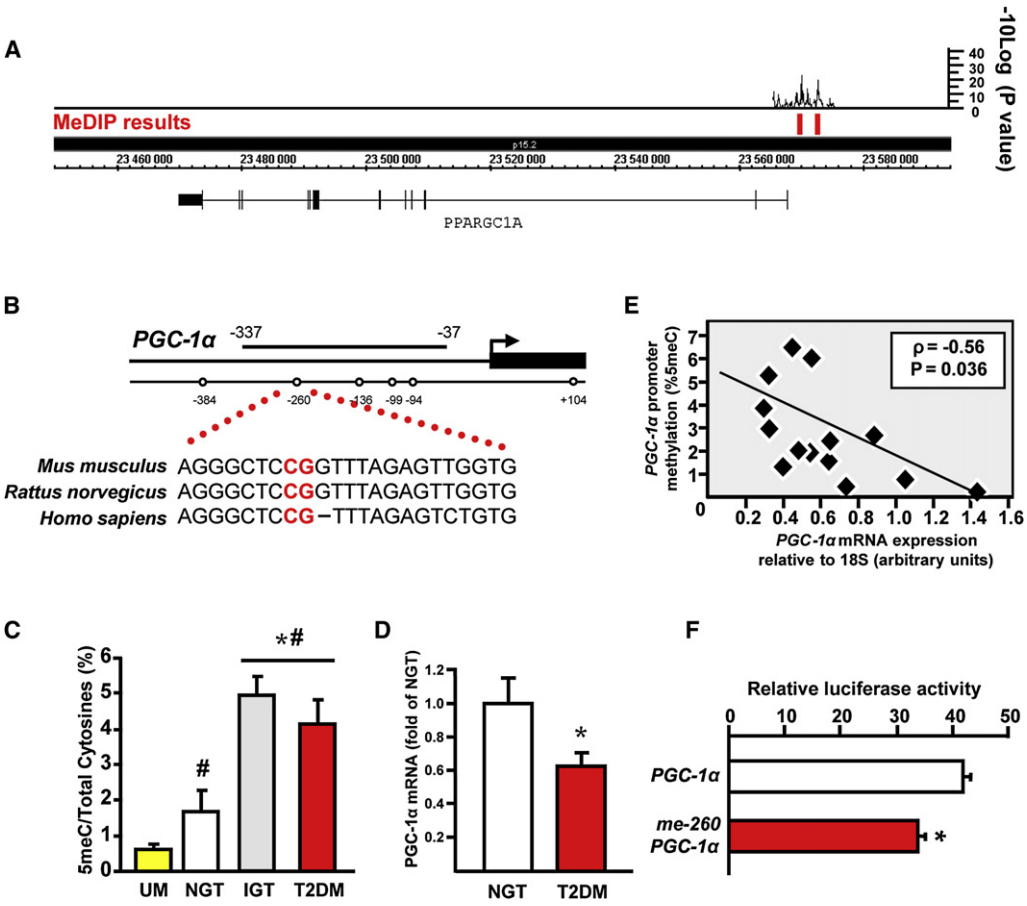

Figure 1. *PGC-1α* Promoter Is Hypermethylated in T2DM Patients

(A) Genomic localization and representation of the microarray signal using the Integrated Genome Browser for the *PGC-1α* gene (PPARGC1A). Red bars represent MeDIP result from patients with normal glucose tolerance (NGT, n = 10) versus with type 2 diabetes (T2DM, n = 10), with a p value < 0.05.

(B) Graphic representation of the bisulfite-sequenced portion on the *PGC-1α* gene. The transcription start site (arrow) and first exon (black box) are shown. The CpG sites within the bisulfite-sequenced region are represented (open circles). Expanded *Mus musculus*, *Rattus norvegicus*, and *Homo sapiens* sequence surrounding the −260 cytosine is shown.

(C) Methylation analysis of the *PGC-1α* promoter by bisulfite sequencing; percentage of cytosine methylation for unmethylated sequence (UM), in people with normal glucose tolerance (NGT, n = 7), impaired glucose tolerance (IGT, n = 8), or type 2 diabetes (T2DM, n = 7). Results are mean ± SEM for n = 7 individuals (*p < 0.05 versus NGT, #p < 0.05 versus UM).

(D) Real-time PCR quantification of *PGC-1α* mRNA expression in *vastus lateralis* biopsies from NGT (n = 7) or T2DM (n = 7) subjects. Data are normalized to 18S mRNA and expressed as fold of NGT. Results are mean ± SEM for n = 7 individuals (*p < 0.05).

(E) *PGC-1α* methylation levels are negatively associated with PGC-1α expression levels. Pearson correlation coefficient (ρ) and P value are indicated in upper white box.

(F) Suppression of the *Pgc-1α* promoter activity by cytosine −260 methylation. The pCpG vector containing unmethylated (*PGC-1α*) or in vitro-methylated portion of *PGC-1α* promoter (me-260 *PGC-1α*) was cotransfected with empty pGL4 into 3T3-L1 Adipocytes. *Firefly* luciferase activity was assayed at 48 hr after transfection and normalized to *Renilla* luciferase activity. Results are mean ± SEM for three independent experiments (*p < 0.05).

associated with methylation events (Bjornsson et al., 2008; Issa et al., 1994; Siegmund et al., 2007). Oxidative capacity, as measured by VO_2 max, and body mass index (BMI) were not significantly different between the groups studied. To identify candidate genes for methylation events, *vastus lateralis* muscle biopsies obtained from the volunteers were studied. Samples enriched for methylated DNA fragments were probed on an array covering approximately 7.5 kb upstream through 2.45 kb downstream of referenced 5′ transcription start sites. Of 25,500 promoter regions represented on the array, 838 were differentially methylated ($p < 0.05$) in skeletal muscle obtained from NGT versus T2DM subjects. To identify groups of genes with similar changes in methylation in skeletal muscle from T2DM patients, we defined the biological processes of the identified genes using a gene ontology classification (Dennis et al., 2003). We ranked genes by the level of statistical significance (p values) and number of genes in the gene ontology clusters (Table S2). We revealed 44 positive genes as classified in the mitochondrion ontology (Table S3). Of interest, the PGC-1α promoter was hypermethylated in skeletal muscle from T2DM patients compared to NGT subjects ($p < 0.05$) (Figure 1A).

We validated the MeDIP result for *PGC-1α* using bisulfite sequencing. Genomic DNA was extracted from *vastus lateralis* muscle biopsies obtained from NGT, impaired glucose-tolerant

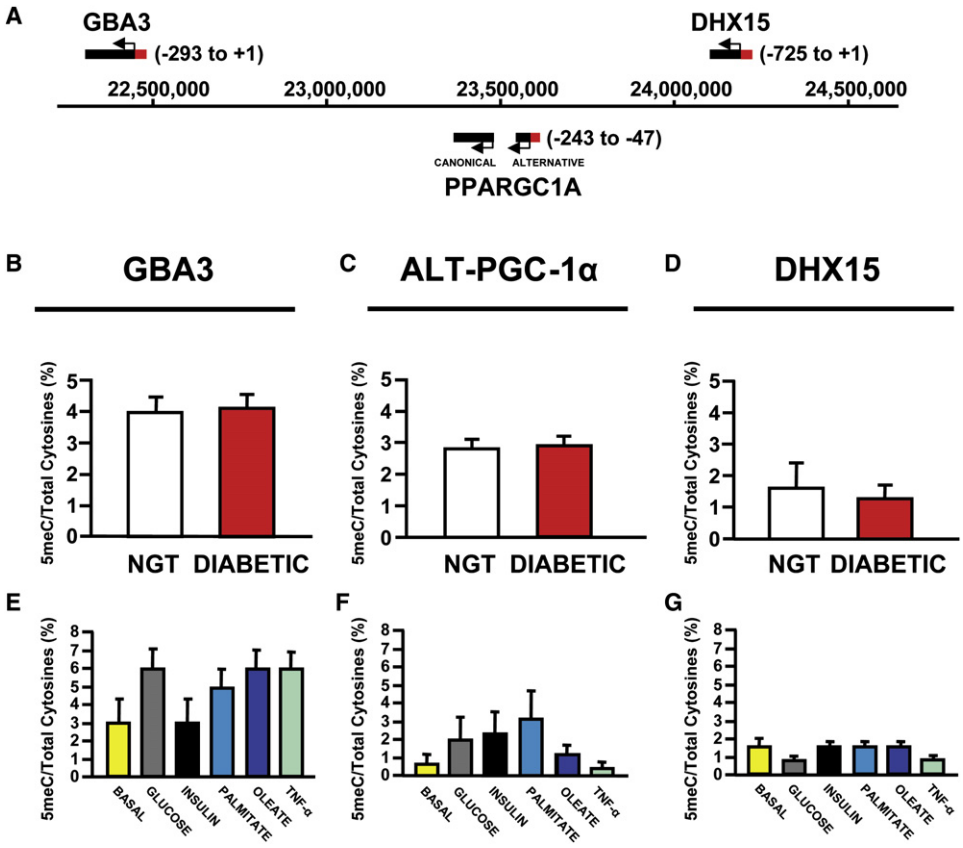

Figure 2. Methylation Analysis of Genes Flanking *PGC-1α* by Bisulfite Sequencing

(A) Graphic representation of the genomic localization of the alternative *PGC-1α* promoter (ALT), DHX15, and GBA3 on chromosome 4. The transcription start site (arrow), transcribed portion of the genes (black box), and sequenced promoters (red box) are shown. Genomic coordinates are indicated.

(B–D) Percentage of cytosine methylation assessed in skeletal muscle biopsies from NGT or T2DM subjects for GBA3 (B), ALT-*PGC-1α* (C), and DHX15 (D). Results are mean ± SEM for n = 8 individuals.

(E–G) Bisulfite sequencing quantification of GBA3 (E), ALT-*PGC-1α* (F), and DHX15 (G) promoter methylation levels in primary myotubes treated with glucose (20 mM), insulin (120 nM), palmitate (0.5 mM), oleate (0.5 mM), or TNF-α (1 μM) for 48 hr. Results are mean ± SEM for 30 independent clones.

(IGT), or T2DM subjects (Table S1). Bisulfite sequencing was performed on a portion of the promoter encompassing −337 to −37 relative to the +1 transcription start site of *PGC-1α* gene in each individual (Figures 1B and S1). The efficiency of the bisulfite conversion was compared to the unmethylated fragment of the region of interest of the *PGC-1α* promoter (Figure 1C). We found a 2.7- and 2.2-fold increase in unconverted cytosines on the *PGC-1α* promoter of IGT and T2DM patients, respectively, compared to NGT subjects (Figure 1C). An alternative promoter of human *PGC-1α* has recently been identified (Yoshioka et al., 2009). Methylation of a portion encompassing −243 to −47 relative to the +1 transcription start site of *PGC-1α* alternative promoter was similar in NGT as compared to T2DM subjects. Through further bisulfite sequencing of *DHX15* and *GBA3,* two genes proximal to *PGC-1α*, we reveal that hypermethylation in T2DM is not broadly altered on a wide portion of the chromatin, but is specific to the canonical *PGC-1α* promoter (Figure 2). Most of the methylated cytosines were found within non-CpG dinucleotides (Figure S1). Of interest, the hypermethylation pattern observed in the T2DM patients was unrelated to family history of the disease. Our findings highlight the potential physiological importance of non-CpG methylation in human skeletal muscle, since non-CpG methylation has been almost exclusively reported in plants and embryonic stem cells (Grandjean et al., 2007; Meyer et al., 1994; Ramsahoye et al., 2000).

PGC-1α Methylation Controls *PGC-1α* Expression

Given that DNA methylation located within or close to the 5′ region of genes has been associated with regulation of gene expression (Costello and Plass, 2001), we next assessed whether *PGC-1α* mRNA expression was altered in skeletal muscle biopsies from NGT and T2DM subjects. *PGC-1α* mRNA content was decreased 38% in T2DM patients (Figure 1D) and negatively correlated with promoter methylation ($\rho = -0.56$, $p = 0.036$) (Figure 1E). Further investigation of the role of *PGC-1α* promoter methylation on gene activity using a gene reporter assay revealed that in vitro methylation of a single cytosine residue (located −260 relative to the +1 transcription start site) caused a marked reduction of gene activity (Figure 1F). Several lines of evidence suggest that insulin resistance and T2DM are associated with decreased skeletal muscle mitochondrial function, which can reduce cellular and whole-body oxidative capacity (Kelley et al., 2002; Simoneau

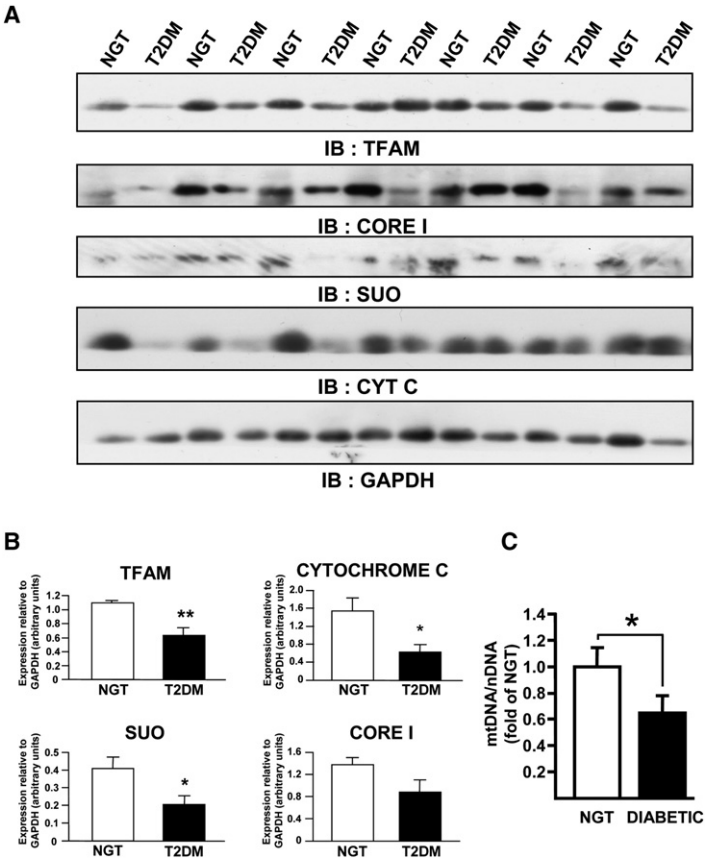

Figure 3. Decreased Mitochondrial Markers in Type 2 Diabetic Patients

(A) Expression of mitochondrial proteins. Western blot analysis of individual content of TFAM, core I (or complex III), succinate-ubiquinol reductase (SUO or complex II), and cytochrome C (CytC) is shown.

(B) Quantification of western blot was normalized by GAPDH expression in NGT (n = 7, open box) and T2DM (n = 7, black box) subjects. Results are mean ± SEM (*p < 0.05, **p < 0.005).

(C) Decreased mtDNA content in T2DM patients. Quantification of mtDNA to nDNA ratio using real-time PCR in NGT (n = 8, open box) and T2DM (n = 8, black box). Results are mean ± SEM (*p < 0.05).

and Kelley, 1997). Reductions in mitochondrial density have also been proposed as a primary cause of mitochondrial dysfunction in insulin-resistant states (Boushel et al., 2007). Here, we show that *PGC-1α* promoter methylation was negatively correlated with mitochondrial DNA (mtDNA) content, as measured by ratio of mtDNA to nuclear DNA (nDNA) using real-time quantitative PCR ($\rho = -0.55$, $p = 0.043$) (Figure S2).

Decreased Mitochondrial Content in Patients with T2DM

PGC-1α is a key factor that coordinately regulates the expression of a subset of mitochondrial genes and participates in the overall mitochondrial function in the cell (Lin et al., 2005). To examine whether mitochondrial content is altered in skeletal muscle from T2DM patients, proteins from the mitochondrial respiratory chain were measured in crude lysates. The relative amounts of succinate-ubiquinol reductase (SUO or complex II), core I (complex III), and cytochrome C (CytC) were significantly decreased in T2DM patients compared with NGT subjects (Figures 3A and 3B). Additionally, the level of expression of the mitochondrial transcription factor A (TFAM), a key protein in the regulation of mtDNA quantity, was significantly decreased in T2DM compared with NGT subjects (Figures 3A and 3B). The ratio of mtDNA per nucleus was decreased 22% in T2DM patients (Figure 3C). Ultrastructural analysis of skeletal muscle obtained from each cohort further supports these findings, as both mitochondrial number and area were significantly reduced ($p < 0.001$) in T2DM patients compared with NGT subjects (Figures 4A–4C). Thus, mitochondrial markers were decreased in skeletal muscle from T2DM patients, indicative of altered mitochondrial content in this cohort.

Role of Free Fatty Acids and TNF-α in *PGC-1α* Methylation

Alterations in the extracellular milieu, including hyperglycemia, hyperinsulinemia, elevated free fatty acids, and elevated cytokines, can cause peripheral insulin resistance in T2DM. To investigate whether these external factors directly and acutely alter the methylation status, we used primary human skeletal muscle cells derived from *vastus lateralis* biopsies obtained from NGT men and screened for putative factors involved in *PGC-1α* methylation. Primary human skeletal muscle cultures were incubated for 48 hr with various factors known to induce insulin resistance (Figure 5A). TNF-α, palmitate, and oleate induced hypermethylation of the *PGC-1α* promoter, whereas high glucose or insulin concentrations were without effect. Similar to our results in muscle tissue, bisulfite sequencing revealed that the majority of the methylated cytosines were located outside of CpG nucleotides (Figure 5B). We next evaluated whether these changes occurred as a consequence of whole-genome methylation using luminometric methylation assays (LUMA). Upon palmitate treatment, we found that both global CpA and CpT methylation within 5′-CCA/TGG-3′ was increased from 1.6% to 4.2% (Figure 6A), although CpG methylation within the 5′-CCGG-3′ sequence was unaltered (Figure 6B). In *vastus lateralis*, we observed similar CpG and non-CpG levels (Figures 6C and 6D). These results provide further evidence of high non-CpG methylation in human skeletal muscle. Moreover, global methylation levels were unchanged in T2DM patients (Figures 6C and 6D), suggesting that hypermethylation is gene specific. Collectively, these data provide evidence that free fatty acids acutely induce non-CpG methylation at the *PGC-1α* promoter and at the whole-genome level in primary human myocytes.

DNMT3B Is Involved in Palmitate-Induced DNA Methylation in Human Muscle Cells

In mammals, three functional DNA methyltransferase (DNMT) isoforms have been identified: DNMT1, DNMT3A, and DNMT3B. To identify whether DNMTs are involved in palmitate-induced *PGC-1α* promoter methylation, we selectively silenced DNMT1,

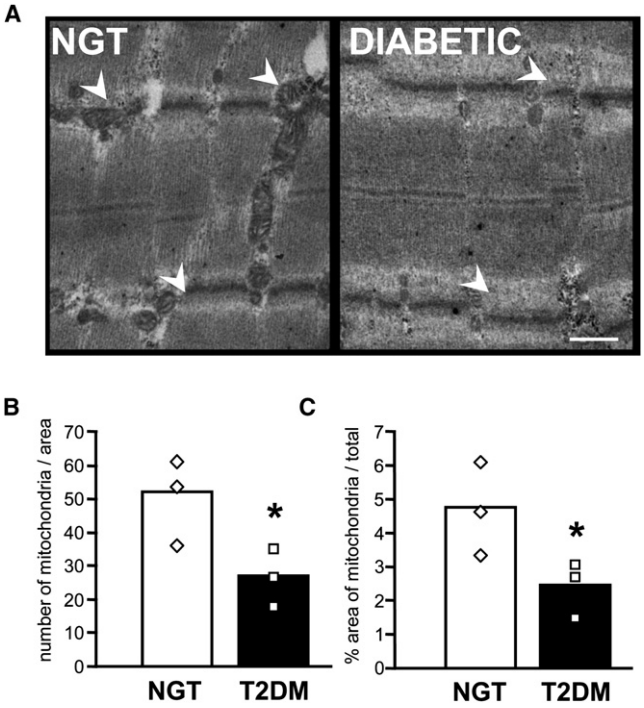

Figure 4. Decreased Mitochondrial Content in Type 2 Diabetic Patients

(A–C) Mitochondrial ultrastructure was examined in skeletal muscle from NGT (n = 3) and T2DM (n = 3) subjects by transmission electron microscopy. Representative images of samples from an NGT subject and a T2DM patient are shown (A). Note the mitochondria located between contractile units (arrows). Images are of type I fibers (note the thick Z-line); scale bar represents 500 nm. The number (B) and area (C) of mitochondria were determined from images captured at 2800× with an area of 7.2 μm^2. Bars represent the mean of all images counted, and points represent means of individual subjects. Area data are expressed in mitochondria area per total image area (*p < 0.001).

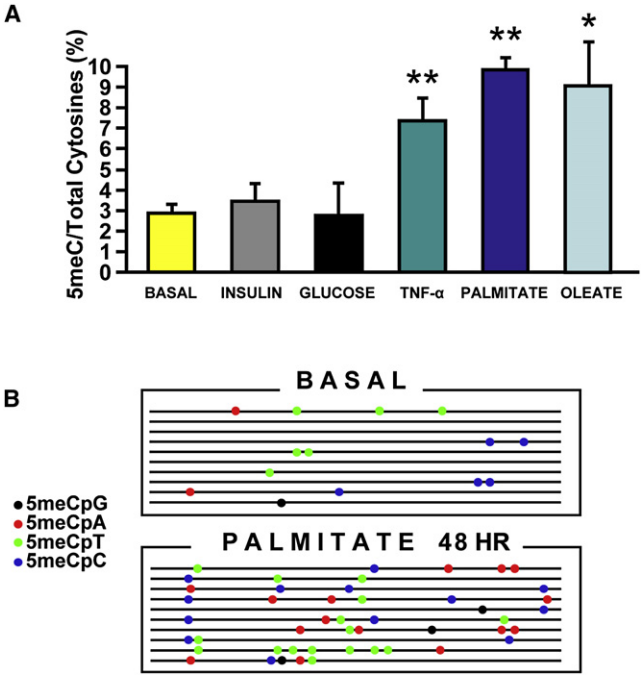

Figure 5. Free Fatty Acids Induce *PGC-1α* Promoter Methylation in Primary Human Myocytes

(A) Bisulfite sequencing quantification of *PGC-1α* promoter methylation levels in cells treated with insulin (120 nM), glucose (20 mM), TNF-α (1 μM), palmitate (0.5 mM), or oleate (0.5 mM) for 48 hr. Results are mean ± SEM for 30 independent clones (*p < 0.05 versus basal).

(B) Visualization of bisulfite sequencing results as analyzed by MethTools 2.0 (Grunau et al., 2000) (http://genome.imb-jena.de/methtools/) in basal conditions (upper panel) or after 48 hr of palmitate treatment (lower panel).

DNMT3A, and DNMT3B in human primary muscle cells. Gene silencing of either DNMT1 or DNMT3A failed to rescue palmitate-induced downregulation of *PGC-1α* mRNA and mitochondrial gene expression (Figure S3). In contrast, silencing of DNMT3B 43% (Figure 7A) prevented palmitate-induced *PGC-1α* promoter methylation (Figure 7B). Furthermore, the palmitate-induced reduction of mtDNA content, as evaluated by the mtDNA to nDNA ratio, was partly prevented by DNMT3B silencing (Figure 7C). Quantitative PCR was also performed to detect any variation in the expression of genes related to mitochondrial function and biogenesis (Figure 7D). DNMT3B silencing prevented the palmitate-induced downregulated mRNA expression of *PGC-1α*, *TFAM*, citrate synthase (CS), and carnitine palmitoyltransferase (CPT)-2. Conversely, the effect of palmitate treatment to upregulate mRNA expression of *CPT-1* and *CytC* was unaltered by DNMT3B silencing. Nuclear respiratory factor 1 (NRF-1) was unaltered by either palmitate treatment or DNMT3B silencing. Thus, the expression of a subset of genes important for mitochondrial regulation is downregulated following palmitate exposure in a DNMT3B-dependent manner. We cannot directly link *PGC-1α* to the regulation of these genes, because changes in gene expression could have been caused by a direct effect of palmitate. These genes may themselves be targets of dynamic regulation via methylation, or they may be regulated as a consequence of the reduction in *PGC-1α* expression. For example, our MeDIP analysis revealed *TFAM* and *CPT-2* are hypermethylated in skeletal muscle from T2DM patients (data not shown). These results provide evidence that DNMT3B plays a role in palmitate-induced DNA methylation and the control of mitochondrial marker gene expression in human skeletal muscle cells. However, protein content of DNMT isoforms were unchanged following 48 hr exposure of human myocytes to high concentrations of glucose, insulin, palmitate, oleate, or TNF-α (Figure S4A). In skeletal muscle from NGT and T2DM subjects, quantitative analysis of DNMT isoforms using RT-PCR revealed mRNA expression of *DNMT3B* (normalized to actin) was increased in T2DM versus NGT subjects (378 ± 42 versus 215 ± 46 arbitrary units, respectively; $p < 0.05$). In contrast, mRNA expression of *DNMT1* (1685 ± 201 versus 1580 ± 315 arbitrary units) and *DNMT3A* (6168 ± 633 versus 6161 ± 857 arbitrary units) was unchanged between T2DM and NGT subjects, which further supports a role of *DNMT3B* in increased methylation levels. However, protein content was unaltered between T2DM and NGT subjects (Figure S4B). Thus, collectively, our results suggest that enzymatic activation of DNMT3B, rather than changes in protein expression, is involved in hypermethylation of the *PGC-1α* promoter.

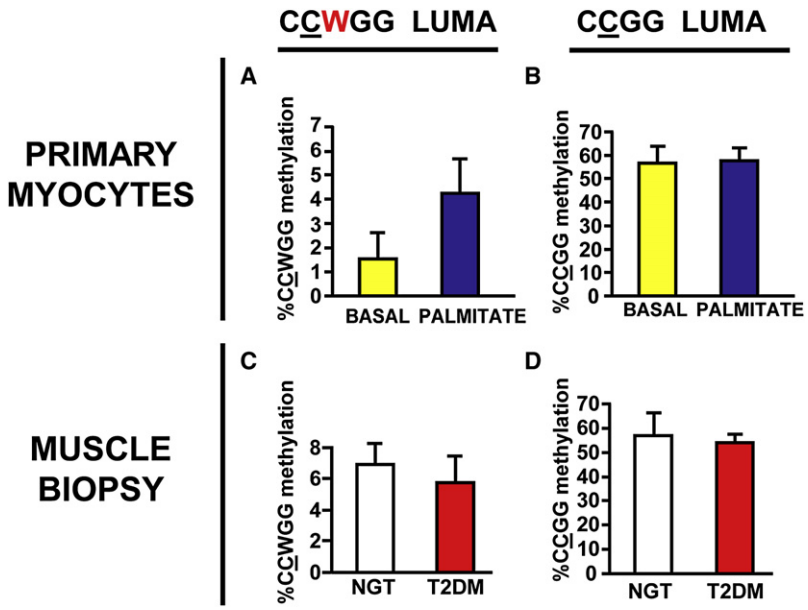

Figure 6. Luminometric Assay Analysis of Global DNA Methylation

(A–D) Global CpG and non-CpG methylation analysis in primary human myocytes exposed to palmitate is shown in (A) and (B). Global CpG and non-CpG methylation analyses in *vastus lateralis* biopsies from people with NGT or T2DM are shown in (C) and (D). Genomic DNA was digested using the restriction enzymes Psp6I and AjnI. The ratio (Psp6I)/(AjnI) was plotted to a standard curve to determine the percent CCWGG methylation levels. Results are mean ± SEM (A and C). Genomic DNA was also digested using the restriction enzymes MspI, HpaII, and EcoRI. The value [1 − (HpaII/EcoRI)/(MspI/EcoRI)] × 100 was used as percent CCGG methylation level. Results are mean ± SEM (B and D).

DISCUSSION

Mitochondrial dysfunction has been proposed to contribute to impaired fat oxidation and excess lipid storage in skeletal muscle (Morino et al., 2006). Here, we provide evidence for epigenetic modifications on the *PGC-1α* promoter in skeletal muscle from T2DM patients using genome-wide promoter screening of DNA methylation. PGC-1α is a master regulator of mitochondrial biogenesis and function (Wu et al., 1999). Hypermethylation of the *PGC-1α* promoter was associated with reduced *PGC-1α* expression and implicates a mechanism for decreased mitochondrial content in T2DM.

Downregulation of *PGC-1α* expression in T2DM subjects was previously reported (Mootha et al., 2003). Consistent with the notion that mitochondrial oxidative capacity is impaired in T2DM, we report that *PGC-1α* and several mitochondrial markers, including TFAM, CytC, SUO, and core I, as well as mtDNA/nDNA and mitochondrial size and number, are reduced. In the present study, we couple *PGC-1α* promoter hypermethylation with reduced mitochondrial density and provide a potential mechanism for mitochondrial dysfunction in T2DM. Whether alterations in mitochondrial function or PGC-1α levels are directly linked to insulin resistance or diabetes remains unclear. However, we observed a negative association between *PGC-1α* promoter methylation and mRNA levels and also provide evidence that DNA methylation influences *PGC-1α* promoter activity. Furthermore, the *PGC-1α* promoter is hypermethylated in skeletal muscle from IGT subjects, indicating this may be an early event in the pathogenesis of insulin resistance in T2DM. Nevertheless, reduced skeletal muscle *PGC-1α* mRNA expression has been noted in some (Patti et al., 2003), but not all (Karlsson et al., 2006), nondiabetic family history-positive subjects, despite impairments in mitochondrial function (Morino et al., 2005). Thus, additional factors may also contribute to the reduced mitochondrial content in history-positive nondiabetic subjects and T2DM patients. Indeed, changes in *PGC-1α* mRNA expression and mitochondrial function may be related to alterations in physical activity or nutritional status between the NGT and T2DM subjects, rather than diabetes per se. Whether methylation of the *PGC-1α* promoter is an early pathogenic event in the pathogenesis of insulin resistance in T2DM or a more generalized consequence causally related to features of IGT and T2DM requires further evaluation.

Lipid overload can impair skeletal muscle oxidative capacity and increase intramuscular triglyceride content, thereby providing a role for nutritional factors in the development of peripheral insulin resistance in T2DM (Borkman et al., 1993; Dobbins et al., 2001; Valtueña et al., 1997). The hypermethylation of the *PGC-1α* promoter upon free fatty acid exposure is compatible with previous evidence of a close relationship between *PGC-1α* mRNA levels in cultured myotubes and circulating fatty acid levels of the donor and strongly implicates fatty acids in the epigenetic modification of *PGC-1α* mRNA expression (Staiger et al., 2006). We also observed *PGC-1α* promoter hypermethylation upon TNF-α exposure. Excessive levels of free fatty acids and TNF-α stimulate the accumulation of the sphingolipid ceramide and various ceramide metabolites (Summers and Nelson, 2005), which potentially forms a link between free fatty acid and TNF-α-induced DNA methylation.

Several lines of evidence support a role for epigenetic processes in the regulation of metabolic disease, indicating a strong link between gene and environment. Changes in DNA methylation levels are associated with alterations in the expression of genes involved in mitochondrial function, including cytochrome c oxidase subunit VIIa polypeptide 1 (*COX7A1*), NADH dehydrogenase (ubiquinone) 1 beta subcomplex 6 (*NDUFB6*), and *PGC-1α* in humans (Ling et al., 2007, 2008; Rönn et al., 2008). Moreover, the lysine (K)-specific demethylase 3A (Kdm3a) has been implicated in the transcriptional regulation of PPARα (Tateishi et al., 2009). From our MeDIP screen of skeletal muscle biopsies, we retrieved numerous genes with differential methylation status in skeletal muscle from T2DM versus NGT volunteers, including subsets of genes involved in primary metabolic processes and mitochondrial function. Future efforts in systems biology will be required to understand the complexity of gene-environment interactions in health and disease. DNA

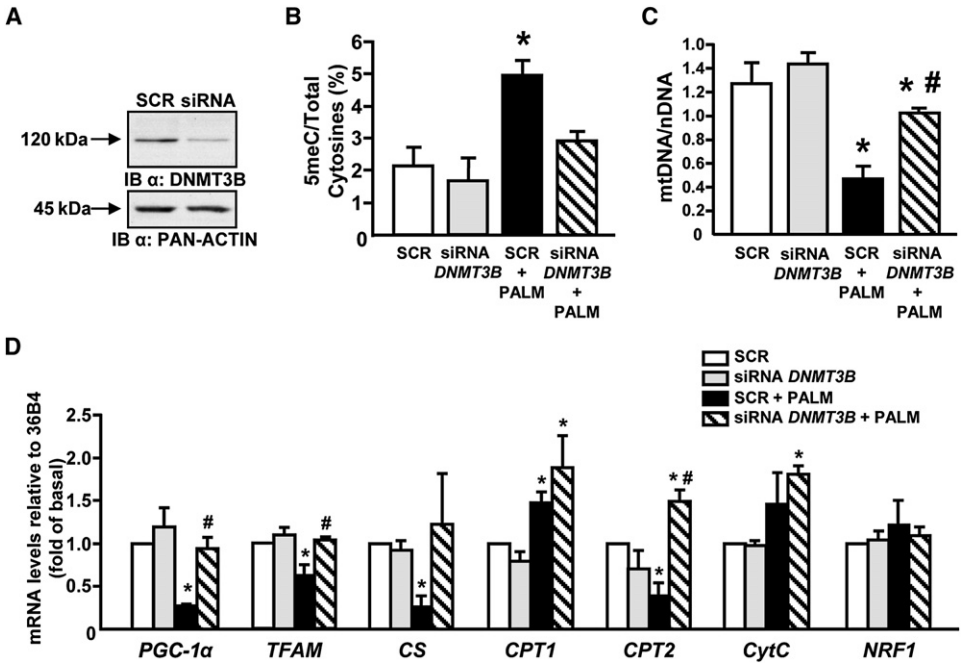

Figure 7. DNMT3B Is Involved in the Palmitate-Induced Decrease of mtDNA

(A) Specific siRNA-mediated depletion of DNMT3B protein was confirmed relative to the scrambled siRNA by western blot analysis 48 hr after transfection of siRNA. Pan-actin was used as a loading control. A representative image is shown.

(B–D) Analysis in cells transfected with the scrambled siRNA (SCR) after palmitate treatment in primary human myocytes previously transfected with the scrambled siRNA (SCR + PALM) or the *DNMT3B* siRNA (siRNA *DNMT3B* + PALM). DNMT3B silencing prevents palmitate-induced *PGC-1α* methylation (B). Methylation analysis of the *PGC-1α* promoter is performed by bisulfite sequencing. Results are mean ± SEM for ten independent clones and for three different subjects (*$p < 0.05$ versus scr.). DNMT3B silencing partially reverses the palmitate-induced decrease in mtDNA content (C). The nDNA versus mtDNA ratio was determined in primary human myocytes using quantitative PCR. Results are mean ± SEM for three different subjects (*$p < 0.05$ versus scramble; #$p < 0.05$ versus scramble + palmitate). Relative expression of genes in mitochondrial function after *DNMT3B* silencing is shown in (D). Quantitative PCR was used to determine the mRNA levels of *PGC-1α*, *TFAM, CS*, *CPT-1*, *CPT-2*, *CytC*, and *NRF-1*. Results are mean ± SEM for three different subjects (*$p < 0.05$ versus scramble; #$p < 0.05$ versus scramble + palmitate).

methylation may provide a mechanism to link environmental factors with the long-term establishment of T2DM.

Rapid changes in the DNA methylation pattern occur during early mammalian development or during cell division (Adams, 1971; Li, 2002). Here, we show that DNA methylation can be acutely induced in somatic cells. *PGC-1α* promoter hypermethylation in response to TNF-α or free fatty acids occurred in a time-dependent manner (data not shown), indicating dynamic DNA hypermethylation occurs in differentiated, nondividing cells. Discovery of whether DNA methylation changes are involved in the adaptation to the extracellular environment requires further investigation. However, the absence of an association between *PGC-1α* methylation levels and family history of diabetes in our study provides evidence that *PGC-1α* hypermethylation in T2DM may occur as a consequence of the deleterious metabolic milieu directly on somatic cells, rather than through inherited factors.

DNA methylation in mammals is predominantly reported on cytosines of the dinucleotide sequence CpG. However, non-CpG methylation was described at measurable levels in embryonic stem cells (Grandjean et al., 2007; Ramsahoye et al., 2000). Using various approaches, we provide evidence that non-CpG methylation is readily observed in human skeletal muscle. Of interest, we observed greater non-CpG methylation levels on *PGC-1α* and *TFAM* (data not shown) promoters compared to global levels. Although further investigations are necessary to determine if non-CpG methylation is more concentrated to promoter regions within the genome, our finding that 7% of cytosines within the sequence CCAGG or CCTGG are methylated in human skeletal muscle suggests that further attention should be given to non-CpG methylation when using current DNA methylation analysis techniques. We identified *PGC-1α* by MeDIP. Given that the *PGC-1α* promoter contains a higher proportion of non-CpG sites (4 CpG and 56 non-CpG within the region analyzed), non-CpG methylation is likely to contribute to a greater extent in *PGC-1α* promoter precipitation. This raises the importance of considering non-CpG methylation when interpreting MeDIP analysis.

Here, we highlight that changes in the metabolic environment lead to a rapid epigenetic modulation of *PGC-1α*, which has been implicated in the development of T2DM and related metabolic disorders. T2DM remains a complex and multifaceted disease, the exact cause of which has yet to be resolved. While obesity and genetic predisposition can contribute to the development of T2DM, diet and physical activity can also have a positive impact on insulin sensitivity. Epigenetic modifications provide a mechanism by which external environmental factors can modify genetic predisposition for health and disease.

EXPERIMENTAL PROCEDURES

Reagents, Tissue Preparation, and Cell Culture

The following antibodies were used for the western blot analysis: mtTFA (A-17) and GAPDH (FL-335) were purchased from Santa Cruz Biotechnology, Inc. (Santa Cruz, CA); SUO and core I (16D10) were purchased from Molecular Probes Invitrogen AB, Sweden; CytC was from BD Biosciences, Inc. (Franklin Lakes, NJ). The DNMT1 antibody was obtained from Abcam (Cambridge, UK); DNMT3A and DNMT3B antibodies were obtained from Cell Signaling Technology (Danvers, MA). Sodium betabisulfite, hydroquinone, TNF-α, oleate and palmitate were purchased from Sigma-Aldrich (Stockholm).

Study Participants

Experiments were performed with approval from the local ethics committee. All studies were performed according to the Declaration of Helsinki. Informed written consent was obtained from all participants before testing was initiated. Clinical characteristics of NGT (n = 17), IGT (n = 8), and T2DM (n = 17) participants are presented (Table S1). T2DM patients were treated with diet, sulfonylureas, or metformin. Individuals taking β-adrenergic receptor blockers, ACE inhibitors, or hormonal therapy were excluded from the study.

Clinical Analysis

Serum insulin level was measured with a commercially available fluoroimmunoassay (Delphia; Perkin Elmer; Waltham, MA). Plasma glucose was measured using a glucose oxidase method (Beckman Coulter; Fullerton, CA), and HbA1c was assessed by HPLC using an autoanalyzer (RG41 5RA; Menarini Diagnostics; Berkshire, UK). Plasma triacylglycerol was measured using enzymatic methods (Roche Diagnostics; Basel, Switzerland). Peak pulmonary oxygen uptake rate (VO_2 peak) was determined by an incremental exercise test to volitional fatigue on an electromagnetically braked cycle ergometer (SensorMedics; Yorba Linda, CA). Expired oxygen and carbon dioxide content was measured with oxygen and carbon dioxide analyzers, respectively. Ventilation was measured by a turbine flow transducer. Peak VO_2 was considered as the highest VO_2 attained during the latter stages of the test.

Skeletal Muscle Biopsy

Skeletal muscle biopsies (50–100 mg) were obtained under local anesthesia (Lidokain hydrochloride 5 mg/ml) from the *vastus lateralis* portion of the *quadriceps femoris* using a Weils-Blakesly contochome. Biopsy samples for mRNA, DNA, and protein analysis were immediately frozen and stored in liquid nitrogen until analysis. For ultrastructural examination, skeletal muscle biopsies from a subgroup of the NGT and T2DM cohort (NGT, n = 3; T2DM, n = 3) were fixed in 3% glutaraldehyde plus 300 mM sucrose in 0.1 M cacodylate buffer (pH 7.4) overnight, postfixed for 1 hr in 1% osmium tetroxide, dehydrated through a graded alcohol series, and embedded in Durcupan resin (Sigma). Ultrathin 70 nm sections were placed on copper mesh grids (Electron Microscopy Science; Hatfield, PA), counterstained with 2% uranyl acetate and lead citrate, and examined with a Morgagni 268 transmission electron microscope. Ten random images were captured using the AMT camera system (Advanced Microscopy Techniques; Danvers, MA) at 2800×. Total mitochondrial number and volume density were determined for each image.

Human Skeletal Muscle Cell Culture

Vastus lateralis muscle biopsies were collected in cold phosphate-buffered saline (PBS) supplemented with 1% PeSt (100 U ml^{-1} penicillin/100 μg ml^{-1} streptomycin). Biopsies were dissected free from visible connective and fat tissue, minced finely, mixed with trypsin-EDTA, and incubated with gentle agitation at 37°C for 5 min. Thereafter, undigested tissue was allowed to settle, and the supernatant containing liberated satellite cells was collected and mixed with growth media (DMEM/Ham's F12 supplemented with 20% FBS, 1% PeSt, 1% Fungizone). The remaining tissue was repeatedly digested for another 10 and 15 min. The collected cell suspension was incubated in a noncoated Petri dish for 1 hr to selectively promote adherence of nonmyogenic cells. The supernatant was thereafter transferred to culture flasks, and subcultures 4–5 were used for experiments. At 80% confluence, myotube formation was initiated by lowering serum levels to 2% for 6 days. During the last 48 hr of differentiation, cells were treated with factors known to induce insulin resistance, 120 nM insulin, 20 mM glucose, 1 μM TNF-α, 0.5 mM palmitate, or 0.5 mM oleate.

On the second day of myotube differentiation, siRNAs (80 pmol) were transfected using Lipofectamine 2000 (Invitrogen) in serum and antibiotic-free DMEM. After overnight incubation, cells were washed and put back on differentiation media. Control cultures were transfected with a scrambled siRNA construct encoding a nonspecific siRNA without mammalian homology. The siRNA duplexes were obtained from Sigma Genosys (Sigma-Aldrich, Sweden). The sense sequences were the following: 5′-[dT]GGAAUGGCAGAUGCCAA CAGC[dT]-3′, 5′-[dT]GAAAGCCAAGGUCAUUGCA[dT]-3′, 5′-[dT]GCUACAC ACAGGACUUGAC[dT]-3′ for *DNMT1*, *DNMT3A*, and *DNMT3B*, respectively.

MeDIP Assay

Purified genomic DNA was prepared from cultured cells and tissue samples and digested overnight with AluI restriction enzyme (New England Biolabs; Ipswich, MA) to obtain fragments of 256 base pairs on average. We used 4 μg digested DNA for a standard MeDIP assay, as described (Weber et al., 2005). Denaturated DNA was immunoprecipitated using 10 μg of monoclonal antibody against 5-methylcytidine (Eurogentec; Seraing, Belgium) in 300 μl IP buffer (10 mM sodium phosphate [pH 7.0], 140 mM NaCl, 0.05% Triton X-100) for 5 hr at 4°C and washed three times with 800 μl IP buffer. Immunoprecipitated DNA was recovered with Proteinase K digestion followed by column-based purification (DNA Wizard; Promega; Madison, WI), amplified and hybridized on human tiling array 1.0R chip according to Affymetrix Chromatin Immunoprecipitation Assay protocol (Santa Clara, CA). DNA immunoprecipitates were fragmented and labeled according to recommended protocols (http://www.affymetrix.com/Auth/support/downloads/manuals/chromatin_immun_ChIP.pdf) at the Bioinformatics and Expression Analysis Core Facility, Karolinska Institutet. Hybridization to the GeneChip Human Promoter 1.0R Array as well as scanning of the arrays was performed according to standard Affymetrix protocols.

Analysis of Tiling Array Data

Arrays were quantile-normalized within treatment/control replicate groups and scaled to have a median feature intensity of 130. Using Tiling Array Analysis (TAS version 1.0.15, Affymetrix) software, biological replicates were verified to be very similar to each other and formed relatively tight clusters when plotting log average intensity versus log difference in intensity between the two duplicates (MvA Plot). Probe-level intensities from each group were summarized with TAS by using the "two-sample comparison analysis" option and bandwidth 130. Differentially methylated regions were called by applying a threshold of $p < 0.05$ and by combining neighboring methylated probes allowing a maximal gap of 100 bases and requiring a minimal run of 70 bases. Analysis of *bed* files generated by interval analysis was performed using the integrated genome browser (IGB, Affymetrix). Genes were considered as "positives" when positive array signals were displayed in a region between 7 kb upstream and 3 kb downstream of the +1 transcription start site. In the case of two genes closely neighboring the hit, the gene closer to the hit was taken into account.

Nucleic Acid Purification and Real-Time PCR

DNA from 10–20 mg of *vastus lateralis* muscle was extracted using DNeasy Blood & Tissue columns (QIAGEN). The total amount of DNA recovered was determined by spectrophotometry. For RNA extraction, 10 mg of skeletal muscle tissue was homogenized in 1 ml of TRIzol reagent (Sigma), and RNA was purified according to recommendations of the manufacturer. The RNAs from cultured cells were also purified using TRIzol reagent. One microgram of purified RNA was then treated with DNase I using a DNA-free kit (Ambion) according to the manufacturer's protocol. DNase-treated RNA was used as a template for cDNA synthesis using the SuperScript First-Strand Synthesis System (Invitrogen) with random hexamers. cDNA quantity was measured using real-time PCR with the ABI PRISM 7000 sequence detector system and fluorescence-based SYBR Green technology (Applied Biosystems; Foster City, CA). PCR was performed in a final volume of 25 μl, consisting of diluted cDNA sample, 1× SYBR Green PCR Master Mix (Applied Biosystems), primers optimized for each target gene, and nuclease-free water. All samples were analyzed in duplicates. Primers were designed using Primer Express computer software (Applied Biosystems).

Bisulfite Sequencing

Bisulfite treatment was performed as described (Olek et al., 1996), with the following adaptations: briefly, 1 μg of genomic DNA was embedded in a 2%

low-melting-point agarose solution, and ten beads were formed. A freshly prepared bisulfite solution (4 M sodium betabisulfite, Sigma; 250 mM hydroquinone, Sigma [pH 5.0]) was added to each reaction tube containing one single bead. The reaction mixtures were incubated for 4 hr at 50°C under exclusion of light. Treatment was stopped by equilibrations against 1 ml of Tris-EDTA (TE) (4 × 15 min) followed by desulphonation in 500 μl of 0.2 M NaOH (2 × 15 min). The reaction was neutralized, and beads were washed with 1 ml TE (2 × 15 min). Prior to PCR, beads were equilibrated against 1 ml of ddH2O (2 × 30 min). For amplification of the region from −337 to −37 of *PGC-1α* promoter, the following primers were used: sense 5′ TAT AGT TAT TTT GTT ATG AAA TAG GGA GTT TT G 3′; antisense 5′ CCA ATC ACA TAA CAA AAC TAT TAA AAA ATA A 3′. For amplification of the region from −243 to −47 of the alternative *PGC-1α* promoter, the following primers were used: sense 5′ ATA GGG TTG TTG GAA AGT ATA TGA TAT T 3′; antisense 5′ AAA AAA CAC TCA CAA CAA AAA CTT C 3′. For *DHX15*: sense 5′ TGG AGG TAG TTT TGG TTG TTA TTA T 3′; antisense 5′ CAT TTT AAA ACA AAT AAT TTC TTT TT 3′. For *GBA3*: sense 5′ AAA TGG TTA AAA GTG GTT ATT TTT ATA GAG 3′; antisense 5′ CAA AAC ACC CAT TTA CCT AAT ATT TTA C 3′. The obtained PCR fragments were purified from an agarose gel using MinElute Gel Extraction Kit (QIAGEN) and cloned into pDrive vector using PCR Cloning Kit (QIAGEN), according the manufacturer's protocol. Individual clones were grown and plasmids purified using QIAprep Spin Miniprep Kit (QIAGEN). For each condition, 10–50 clones were sequenced using T7 promoter primer on an ABI 3730xl DNA Analyzer platform at Cogenics (Hope End, UK).

MtDNA Content

The ratio of mitochondrial versus nuclear DNA was determined as described (Walker et al., 2005), with the following adaptations: briefly, 10 μl of purified DNA at 1 ng/μl was amplified in a 25 μl PCR reaction containing 1× SYBR Green Master Mix (Applied Biosystems) and 100 nM of each primer. The amplification was monitored in real-time using the ABI Prism 7000 Real-Time PCR machine (Applied Biosystems). The primers were designed to target nDNA (forward: CTT GCA GTG AGC CGA GAT T A; reverse: GAG ACG GAG TCT CGC TCT GTC) or mtDNA (forward: AAT ATT AAA CAC AAA CTA CCA CCT ACC T; reverse: TGG TTC TCA GGG TTT GTT ATA A).

Western Blot Analysis

Muscle tissue biopsies were freeze-dried and dissected free from blood and connective tissue. Muscles were homogenized in buffer containing 50 mM HEPES (pH 7.6), 150 mM NaCl, 1% Triton X-100, 1 mM Na_3VO_4, 10 mM NaF, 30 mM $Na_4P_2O_7$, 10% (v/v) glycerol, 1 mM benzamidine, 1 mM dithiothreitol, 10 μg/ml leupeptin, 1 mM PMSF, and 1 μM microcystin. Protein was determined by the BCA (bicinchoninic acid) protein assays kit from Pierce (Thermo Fisher Scientific; Waltham, MA). Samples were resuspended in Laemmli buffer, and proteins were separated on 12% SDS-PAGE. Proteins were transferred to polyvinylidenedifluoride membranes (Millipore; Billerica, MA) and subjected to western blot analysis. After incubation with primary antibody, membranes were washed and incubated with secondary antibody linked to horseradish peroxidase (Bio-Rad; Hercules, CA). Multiple film exposures were used to ensure that proteins were detected in linear range of protein band saturation. Results were quantified by densitometry using Gel Doc 1000 imaging system with Molecular Analyst software, version 1.5 (Bio-Rad Laboratories).

LUMA

For LUMA interrogation of CpG methylation within the CCGG sequence, experimental conditions were as previously described (Karimi et al., 2006). Restriction enzymes (HpaII, MspI, and EcoRI) and Tango buffer (33 mM Tris-acetate [pH 7.9], 10 mM Mg-acetate, 66 mM K-acetate, 0.1 mg/ml BSA) were purchased from Fermentas (Stockholm). The PSQ 96 SNP reagents for pyrosequencing were purchased from Biotage (Uppsala). Briefly, 500–1000 ng of genomic DNA was submitted to a double digestion using either HpaII + EcoRI or MspI + EcoRI in Tango buffer (4 hr at 37°C). Following digestion, pyrosequencing annealing buffer was added to each reaction, transferred to 96-well pyrosequencing plates, and analyzed using a pyrosequencer machine with an assay sequence defined as AC/TCGA. Percent CCGG methylation levels were calculated with the following equation: [1 − (HpaII/EcoRI)/(MspI/EcoRI)] × 100.

For LUMA interrogation of CpA or CpT methylation within the CCA/TGG sequence, the restriction enzymes used were Psp6I and AjnI from SibEnzyme Ltd. (Novosibirsk, Russia). Extracted DNA was digested using Psp6I or AjnI in Buffer Y (33 mM Tris-acetate [pH 7.9], 10 mM magnesium acetate, 66 mM potassium acetate, 1 mM DTT) purchased from SibEnzyme. Following digestion, pyrosequencing annealing buffer was added to each reaction, transferred to 96-well pyrosequencing plates, and analyzed using a pyrosequencer machine with an assay sequence defined as AC/TCGA. The ratio (Psp6I)/(AjnI) was plotted to a standard curve in order to determine the percent CCWGG methylation levels.

Statistics

Correlations were calculated using Pearson's coefficient with the SigmaStat 2.03 software (Access Softek; Berkeley, CA). Results are presented as mean ± SEM. Differences between groups were determined by two-tailed unpaired Student's t test. $P < 0.05$ was considered significant.

ACCESSION NUMBERS

MeDIP array results have been archived at EMBL-EBI (http://www.ebi.ac.uk) in a publicly accessible database (MIAMExpress; accession number E-MEXP-2253).

SUPPLEMENTAL DATA

Supplemental Data include four Figures and three tables and can be found online at http://www.cell.com/cell-metabolism/supplemental/S1550-4131(09)00229-0.

ACKNOWLEDGMENTS

The European Foundation for the Study of Diabetes, European Research Council, Swedish Research Council, Swedish Diabetes Association, Strategic Research Foundation, Knut and Alice Wallenberg Foundation, Stockholm County Council, Novo Nordisk Research Foundation, French Foundation for Medical Research, and Commission of the European Communities (contract number LSHM-CT-2004-005272 EXGENESIS and contract number LSHM-CT-2004-512013 EUGENE2) supported this research.

Received: November 19, 2008
Revised: June 17, 2009
Accepted: July 28, 2009
Published: September 1, 2009

REFERENCES

Adams, R.L. (1971). Methylation of newly synthesized and older deoxyribonucleic acid. Biochem. J. *123*, 38P.

Bjornsson, H.T., Sigurdsson, M.I., Fallin, M.D., Irizarry, R.A., Aspelund, T., Cui, H., Yu, W., Rongione, M.A., Ekström, T.J., Harris, T.B., et al. (2008). Intra-individual change over time in DNA methylation with familial clustering. JAMA *299*, 2877–2883.

Borkman, M., Storlien, L.H., Pan, D.A., Jenkins, A.B., Chisholm, D.J., and Campbell, L.V. (1993). The relation between insulin sensitivity and the fatty-acid composition of skeletal-muscle phospholipids. N. Engl. J. Med. *328*, 238–244.

Boushel, R., Gnaiger, E., Schjerling, P., Skovbro, M., Kraunsoe, R., and Dela, F. (2007). Patients with type 2 diabetes have normal mitochondrial function in skeletal muscle. Diabetologia *50*, 790–796.

Cooney, C.A., Dave, A.A., and Wolff, G.L. (2002). Maternal methyl supplements in mice affect epigenetic variation and DNA methylation of offspring. J. Nutr. *132*, 2393S–2400S.

Costello, J.F., and Plass, C. (2001). Methylation matters. J. Med. Genet. *38*, 285–303.

DeFronzo, R.A., Gunnarsson, R., Björkman, O., Olsson, M., and Wahren, J. (1985). Effects of insulin on peripheral and splanchnic glucose metabolism in noninsulin-dependent (type II) diabetes mellitus. J. Clin. Invest. *76*, 149–155.

Dennis, G., Sherman, B.T., Hosack, D.A., Yang, J., Gao, W., Lane, H.C., and Lempicki, R.A. (2003). DAVID: Database for annotation, visualization, and integrated discovery. Genome Biol. *4*, 3.

Dobbins, R.L., Szczepaniak, L.S., Bentley, B., Esser, V., Myhill, J., and McGarry, J.D. (2001). Prolonged inhibition of muscle carnitine palmitoyltransferase-1 promotes intramyocellular lipid accumulation and insulin resistance in rats. Diabetes *50*, 123–130.

Eriksson, J., Franssila-Kallunki, A., Ekstrand, A., Saloranta, C., Widén, E., Schalin, C., and Groop, L. (1989). Early metabolic defects in persons at increased risk for non-insulin-dependent diabetes mellitus. N. Engl. J. Med. *321*, 337–343.

Grandjean, V., Yaman, R., Cuzin, F., and Rassoulzadegan, M. (2007). Inheritance of an epigenetic mark: the CpG DNA methyltransferase 1 is required for de novo establishment of a complex pattern of non-CpG methylation. PLoS ONE *2*, e1136.

Grunau, C., Schattevoy, R., Mache, N., and Rosenthal, A. (2000). MethTools—a toolbox to visualize and analyze DNA methylation data. Nucleic Acids Res. *28*, 1053–1058.

Issa, J.P., Ottaviano, Y.L., Celano, P., Hamilton, S.R., Davidson, N.E., and Baylin, S.B. (1994). Methylation of the oestrogen receptor CpG island links ageing and neoplasia in human colon. Nat. Genet. *7*, 536–540.

Karimi, M., Johansson, S., Stach, D., Corcoran, M., Grander, D., Schalling, M., Bakalkin, G., Lyko, F., Larsson, C., and Ekström, T.J. (2006). LUMA (LUminometric Methylation Assay)–a high throughput method to the analysis of genomic DNA methylation. Exp. Cell Res. *312*, 1989–1995.

Karlsson, H.K., Ahlsén, M., Zierath, J.R., Wallberg-Henriksson, H., and Koistinen, H.A. (2006). Insulin signaling and glucose transport in skeletal muscle from first-degree relatives of type 2 diabetic patients. Diabetes *55*, 1283–1288.

Kelley, D.E., He, J., Menshikova, E.V., and Ritov, V.B. (2002). Dysfunction of mitochondria in human skeletal muscle in type 2 diabetes. Diabetes *51*, 2944–2950.

Keshet, I., Schlesinger, Y., Farkash, S., Rand, E., Hecht, M., Segal, E., Pikarski, E., Young, R.A., Niveleau, A., Cedar, H., et al. (2006). Evidence for an instructive mechanism of de novo methylation in cancer cells. Nat. Genet. *38*, 149–153.

Li, E. (2002). Chromatin modification and epigenetic reprogramming in mammalian development. Nat. Rev. Genet. *3*, 662–673.

Lin, J., Handschin, C., and Spiegelman, B.M. (2005). Metabolic control through the PGC-1 family of transcription coactivators. Cell Metab. *1*, 361–370.

Ling, C., Poulsen, P., Simonsson, S., Rönn, T., Holmkvist, J., Almgren, P., Hagert, P., Nilsson, E., Mabey, A.G., Nilsson, P., et al. (2007). Genetic and epigenetic factors are associated with expression of respiratory chain component NDUFB6 in human skeletal muscle. J. Clin. Invest. *117*, 3427–3435.

Ling, C., Del Guerra, S., Lupi, R., Rönn, T., Granhall, C., Luthman, H., Masiello, P., Marchetti, P., Groop, L., and Del Prato, S. (2008). Epigenetic regulation of PPARGC1A in human type 2 diabetic islets and effect on insulin secretion. Diabetologia *51*, 615–622.

Meyer, P., Niedenhof, I., and ten Lohuis, M. (1994). Evidence for cytosine methylation of non-symmetrical sequences in transgenic Petunia hybrida. EMBO J. *13*, 2084–2088.

Michaud, E.J., van Vugt, M.J., Bultman, S.J., Sweet, H.O., Davisson, M.T., and Woychik, R.P. (1994). Differential expression of a new dominant agouti allele (Aiapy) is correlated with methylation state and is influenced by parental lineage. Genes Dev. *8*, 1463–1472.

Mootha, V.K., Lindgren, C.M., Eriksson, K.F., Subramanian, A., Sihag, S., Lehar, J., Puigserver, P., Carlsson, E., Ridderstråle, M., Laurila, E., et al. (2003). PGC-1alpha-responsive genes involved in oxidative phosphorylation are coordinately downregulated in human diabetes. Nat. Genet. *34*, 267–273.

Morgan, H.D., Sutherland, H.G., Martin, D.I., and Whitelaw, E. (1999). Epigenetic inheritance at the agouti locus in the mouse. Nat. Genet. *23*, 314–318.

Morino, K., Petersen, K.F., Dufour, S., Befroy, D., Frattini, J., Shatzkes, N., Neschen, S., White, M.F., Bilz, S., Sono, S., et al. (2005). Reduced mitochondrial density and increased IRS-1 serine phosphorylation in muscle of insulin-resistant offspring of type 2 diabetic parents. J. Clin. Invest. *115*, 3587–3593.

Morino, K., Petersen, K.F., and Shulman, G.I. (2006). Molecular mechanisms of insulin resistance in humans and their potential links with mitochondrial dysfunction. Diabetes *55* (*Suppl 2*), S9–S15.

Olek, A., Oswald, J., and Walter, J. (1996). A modified and improved method for bisulphite based cytosine methylation analysis. Nucleic Acids Res. *24*, 5064–5066.

Patti, M.E., Butte, A.J., Crunkhorn, S., Cusi, K., Berria, R., Kashyap, S., Miyazaki, Y., Kohane, I., Costello, M., Saccone, R., et al. (2003). Coordinated reduction of genes of oxidative metabolism in humans with insulin resistance and diabetes: Potential role of PGC1 and NRF1. Proc. Natl. Acad. Sci. USA *100*, 8466–8471.

Pembrey, M.E., Bygren, L.O., Kaati, G., Edvinsson, S., Northstone, K., Sjöström, M., and Golding, J. (2006). Sex-specific, male-line transgenerational responses in humans. Eur. J. Hum. Genet. *14*, 159–166.

Ramsahoye, B.H., Biniszkiewicz, D., Lyko, F., Clark, V., Bird, A.P., and Jaenisch, R. (2000). Non-CpG methylation is prevalent in embryonic stem cells and may be mediated by DNA methyltransferase 3a. Proc. Natl. Acad. Sci. USA *97*, 5237–5242.

Rönn, T., Poulsen, P., Hansson, O., Holmkvist, J., Almgren, P., Nilsson, P., Tuomi, T., Isomaa, B., Groop, L., Vaag, A., et al. (2008). Age influences DNA methylation and gene expression of COX7A1 in human skeletal muscle. Diabetologia *51*, 1159–1168.

Siegmund, K.D., Connor, C.M., Campan, M., Long, T.I., Weisenberger, D.J., Biniszkiewicz, D., Jaenisch, R., Laird, P.W., and Akbarian, S. (2007). DNA methylation in the human cerebral cortex is dynamically regulated throughout the life span and involves differentiated neurons. PLoS ONE *2*, e895.

Simoneau, J.A., and Kelley, D.E. (1997). Altered glycolytic and oxidative capacities of skeletal muscle contribute to insulin resistance in NIDDM. J. Appl. Physiol. *83*, 166–171.

Staiger, H., Stefan, N., Machicao, F., Fritsche, A., and Häring, H.U. (2006). PPARGC1A mRNA levels of in vitro differentiated human skeletal muscle cells are negatively associated with the plasma oleate concentrations of the donors. Diabetologia *49*, 212–214.

Summers, S.A., and Nelson, D.H. (2005). A role for sphingolipids in producing the common features of type 2 diabetes, metabolic syndrome X, and Cushing's syndrome. Diabetes *54*, 591–602.

Tateishi, K., Okada, Y., Kallin, E.M., and Zhang, Y. (2009). Role of Jhdm2a in regulating metabolic gene expression and obesity resistance. Nature *458*, 757–761.

Valtueña, S., Salas-Salvadó, J., and Lorda, P.G. (1997). The respiratory quotient as a prognostic factor in weight-loss rebound. Int. J. Obes. Relat. Metab. Disord. *21*, 811–817.

Van den Veyver, I.B. (2002). Genetic effects of methylation diets. Annu. Rev. Nutr. *22*, 255–282.

Walker, J.A., Hedges, D.J., Perodeau, B.P., Landry, K.E., Stoilova, N., Laborde, M.E., Shewale, J., Sinha, S.K., and Batzer, M.A. (2005). Multiplex polymerase chain reaction for simultaneous quantitation of human nuclear, mitochondrial, and male Y-chromosome DNA: application in human identification. Anal. Biochem. *337*, 89–97.

Weber, M., Davies, J.J., Wittig, D., Oakeley, E.J., Haase, M., Lam, W.L., and Schübeler, D. (2005). Chromosome-wide and promoter-specific analyses identify sites of differential DNA methylation in normal and transformed human cells. Nat. Genet. *37*, 853–862.

Wu, Z., Puigserver, P., Andersson, U., Zhang, C., Adelmant, G., Mootha, V., Troy, A., Cinti, S., Lowell, B., Scarpulla, R.C., et al. (1999). Mechanisms controlling mitochondrial biogenesis and respiration through the thermogenic coactivator PGC-1. Cell *98*, 115–124.

Yoshioka, T., Inagaki, K., Noguchi, T., Sakai, M., Ogawa, W., Hosooka, T., Iguchi, H., Watanabe, E., Matsuki, Y., Hiramatsu, R., et al. (2009). Identification and characterization of an alternative promoter of the human PGC-1alpha gene. Biochem. Biophys. Res. Commun. *381*, 537–543.